

# Correspondence

## LDPC Codes for Fading Gaussian Broadcast Channels

Peter Berlin, *Student Member, IEEE*, and  
Daniela Tuninetti, *Member, IEEE*

**Abstract**—In this work, we study coding over a class of two-user broadcast channels (BCs) with additive white Gaussian noise and multiplicative fading known at the receivers only. Joint decoding of low-density parity-check (LDPC) codes is analyzed. The message update rule at the mapping node linking the users' codes is derived and is found to exhibit an interesting soft interference cancellation property. High performance codes are found using the differential evolution optimization technique and extrinsic information transfer analysis adapted to our multiuser setting. The optimized codes have rates very close to the boundary of the achievable region for binary constrained input for both faded and unfaded channels. Simulation results for moderate block lengths show that our codes operate within less than 1 dB of their respective threshold.

**Index Terms**—Broadcast channels (BCs), extrinsic information transfer (EXIT) charts, fading channels, interference cancellation, low-density parity-check (LDPC) codes, sum-product algorithm.

### I. INTRODUCTION

The information-theoretic capacity region of a general broadcast channel [1] (BC) is still unknown 30 years after Cover's original problem formulation (see [2] and references therein for an excellent survey on BCs.) Even for those channels whose ultimate Shannon limit is known, such as degraded [3] and more-capable channels [4], it is unclear whether capacity can be attained by any known class of codes.

In this work, we restrict our attention to two-user BCs with ergodic fading and additive white Gaussian noise. We assume that the fading processes are known at the receivers but unknown at the transmitter. It is well known that superposition coding and stripping at the best receiver is optimal in the unfaded case. However, Tuninetti *et al.* [5] showed that, as opposed to the degraded case, stripping at the best receiver might incur performance degradation in the presence of fading. Instead, the superimposed codewords must be decoded jointly, like in multiple-access channels (MACs) [3]. Notice that superposition is actually sufficient to achieve the degraded message set region [4]. The optimality of superposition coding and joint decoding has been conjectured in [5] but it is as yet unproven. This correspondence does not pursue the capacity region solution, instead it aims at finding code pairs that perform close to the Shannon limit when the codewords are superimposed at the transmitter and jointly decoded at one of the receivers.

In our search for good codes, we concentrate on low-density parity-check (LDPC) codes [6]. We are encouraged by recent results

showing that LDPC codes achieve capacity for binary erasure channels [7]. Moreover, LDPC codes are conjectured [8] to achieve capacity for a broad class of "nonstandard" channels if the binary code is appropriately interfaced with the channel. McEliece's conjecture [8] has been numerically verified for several channel models. We list in the following some of those channel models although, because of space limitation, we just cite the works close to our own.

LDPC codes were shown to achieve reliable transmission at an signal-to-noise ratio (SNR) extremely close to the Shannon limit for memoryless binary-input unfaded Gaussian channels [9]. In [10], it was shown that irregular LDPC codes perform very well on fully interleaved single-user Rayleigh-fading Gaussian channels. In [11], the authors showed that joint decoding of LDPC codes can achieve all points on the dominate face of the capacity region of two-user single-antenna unfaded multiple-access Gaussian channels without the need of time sharing and/or of rate splitting. LDPC codes are further shown to perform well on fading multiple-antenna single-user Gaussian channels [12] and on fading multiple-antenna Gaussian BCs [13]; in both cases, the fading matrix is assumed to be known at the transmitter side as well.

In this work, we investigate the capability of superimposed LDPC codes when transmitted over single-antenna fading BCs. As opposed to single-user and multiple-access settings, the design of codes for two-user BCs must attain two competing goals. On the one hand, one of the two codes must be good for *single-user decoding* (when treating the other code as noise) on the worst channel and, on the other hand, both codes must be good for *joint decoding* on the best channel.

In deriving a multiple-user version of the message-passing decoding algorithm we discover an interesting property of joint decoding on factor graphs. We show that the node linking the users' codes acts as a soft interference canceller. The update rule at such a node amounts to stripping from the received signal the contribution of the other user's codeword as soon as its reliability is sufficiently high, i.e., without requiring complete decoding of one of the codewords.

In order to design the degree distributions of "good" LDPC codes, we first derive the stability condition by extending the approach of [9]. We show that *three* conditions must be met by the candidate degree distributions in order to ensure vanishing bit-error rate (BER).

We then extend the extrinsic information transfer (EXIT) analysis [14] to determine the convergence property of the candidate LDPC ensemble. We model the extrinsic channel [15] to the node linking the users' codes as a binary erasure channel (BEC) in order to quantify, in closed form, the amount of information transferred from one user code to the other.

Finally, we optimize the degree distribution based on the differential evolution algorithm [16]. For the optimized codes, we further analyze the BER performance for finite block length.

The remainder of the correspondence is organized as follows. In Section II, we describe the model for the two-user fading Gaussian BC, we describe an achievable region when the codes are restricted to be binary, we derive the multiple-user version of the message-passing decoding algorithm for decoding LDPC codes, and we show that there exist nodes in the graph that perform interference cancellation; in Section III, we derive the stability condition, we derive the transfer function of the node linking the users' codes, we describe the code optimization technique, and we comment on the found codes and their finite-length performance. Finally, in Section IV, we point out our conclusions.

Manuscript received February 26, 2004; revised October 23, 2004. The material in this correspondence was presented in part at the Workshop on Signal Processing Advances in Wireless Communication, Lisbon, Portugal, July 2004.

P. Berlin is with the École Polytechnique Fédérale de Lausanne (EPFL), Mobile Communications Laboratory (LCM), CH-1015 Lausanne, Switzerland (e-mail: Peter.Berlin@epfl.ch).

D. Tuninetti was with the École Polytechnique Fédérale de Lausanne (EPFL), Mobile Communications Laboratory (LCM), CH-1015 Lausanne, Switzerland. She is now with the Electrical and Computer Engineering Department, University of Illinois at Chicago, Chicago, IL 60612 USA (e-mail: daniela@ece.uic.edu).

Communicated by M. P. Fossorier, Associate Editor for Coding Techniques. Digital Object Identifier 10.1109/TIT.2005.847752

## II. THE TWO-USER FADING GAUSSIAN BCs

In the following we shall indicate with  $\mathcal{N}_R(\boldsymbol{\mu}, \mathbf{K})$  (resp.,  $\mathcal{N}_C(\boldsymbol{\mu}, \mathbf{K})$ ) a vector of real-valued (resp., proper complex-valued) Gaussian random variables with mean  $\boldsymbol{\mu}$  and covariance matrix  $\mathbf{K}$ , with  $I(X; Y)$  the mutual information between  $X$  and  $Y$ , with  $P_X$  the distribution function of  $X$ , and with  $\chi_{\{A\}}$  the indicator function of the event  $A$ .

### A. Channel Model

We focus on the downlink of wireless systems with delay constraints much larger than the fading coherence time and no feedback channel available. We model the channel as a two-user discrete-time complex-valued memoryless fading Gaussian BC with perfect receiver state information whose outputs are

$$\begin{aligned} Y &= (AX + N_y, A) \\ Z &= (BX + N_z, B). \end{aligned} \quad (1)$$

The processes  $A$  and  $B$  are ergodic, instantaneously known at the corresponding receivers, but unknown at the transmitter. The additive noise  $N_u$  at the receiver  $u \in \{y, z\}$  is a proper complex white Gaussian random variable, with zero mean and variance  $N_0$ . The transmit signal  $X$  is subject to the power constraint  $\mathbb{E}[|X|^2] \leq P$ . Without loss of generality, we assume that the single-user capacity of the user- $Y$  channel is larger than the single-user capacity of the user- $Z$  channel, that is,  $C_A(\beta) \geq C_B(\beta)$ ,  $\beta = P/N_0$ , where

$$C_A(\beta) = \mathbb{E}_A [\log_2 (1 + |A|^2 \beta)] \quad (2)$$

and is achieved by  $X \sim \mathcal{N}_C(0, P)$ .

It is easy to verify that the channel in (1) is not degraded [3] for a general distribution on  $(A, B)$ . Although the capacity region is unknown, it was shown [5] that

$$\bigcup_{\alpha \in [0, 1]} \left\{ \begin{array}{l} R_z \leq C_B(\beta) - C_B(\alpha\beta) \\ R_y + R_z \leq C_B(\beta) - C_B(\alpha\beta) + C_A(\alpha\beta) \\ R_y + R_z \leq C_A(\beta) \end{array} \right\} \quad (3)$$

is achievable by

$$X = U\sqrt{\alpha P} + V\sqrt{(1-\alpha)P} \quad (4)$$

for  $U$  and  $V$  independent and identically distributed (i.i.d.)  $\mathcal{N}_C(0, 1)$ . The region in (3) admits the following interpretation. The transmitter *independently* encodes the user- $Z$  message into the codeword  $V$  and the user- $Y$  message into the codeword  $U$ . A fraction  $\alpha$  of the available power  $P$  is assigned to the codeword  $U$  and the remaining fraction  $(1-\alpha)$  to the codeword  $V$ . The actual signal sent over the channel is the *superposition* of  $U$  and  $V$ . User- $Z$  decodes its codeword  $V$  by treating the codeword  $U$  as “noise” while user- $Y$  *jointly* decodes its own message  $U$  and the other user’s message  $V$ , like in a degraded message set setting.

### B. Encoding

Here we are interested in the performance achievable by binary linear codes instead of by Gaussian codes.

In a single-user case, if the input alphabet is constrained to be binary, then the largest achievable mutual information is

$$J_A(\beta) = \mathbb{E}_A [J(|A|^2 \beta)] \quad (5)$$

where the function  $J(x)$  is defined for  $x \geq 0$  as

$$J(x) = \mathbb{E}_{N \sim \mathcal{N}_R(0, 1)} \left[ 1 - \log_2 \left( 1 + e^{-2N\sqrt{2x-4x}} \right) \right] \quad (6)$$

and is achieved by  $X \in \{\pm\sqrt{P}\}$  with equal probability. In the low-SNR regime, i.e.,  $\beta \rightarrow 0$ , binary coding does not incur significant performance degradation with respect to the optimal coding since  $C_A(\beta) - J_A(\beta) = O(\beta^2)$  for every fading distribution [17]. We say

that an ensemble of binary codes approaches the Shannon limit of a Gaussian fading channel, in the limit for infinite block length, if for a transmit SNR  $> \beta$  the average ensemble BER converges to zero and the code rate converges to  $J_A(\beta)$ . Simulations show that optimized ensembles of LDPC codes do approach the Shannon limit, in the above defined sense, of a wide class of Gaussian channels.

As for the single-user case, we expect no significant loss in performance from the use of binary codes in the low SNR regime [17]. We assume that encoding and decoding are performed as for the Gaussian distribution, however,  $(U, V)$  is chosen equally likely in  $\{0, 1\} \times \{0, 1\}$ . In this case, the achievable region is given by (3) but with  $C(\beta)$  in (2) replaced by  $J(\beta)$  in (5). Figs. 1 and 2 show the Gaussian region (dotted line) and the binary region (solid line) for the unfaded case and the Rayleigh-fading case, respectively. For large SNR, the two regions can be far apart.

In the following we assume that the input pair  $(U, V)$  is generated by two independent LDPC codes mapping blocks of  $k_u = nR_u$  i.i.d. equally likely bits into length- $n$  codewords  $\mathbf{c}_u = (c_{u,1}, \dots, c_{u,n})$  for  $u \in \{y, z\}$ . The variable (resp., check) node degree distribution is specified by the polynomial  $\lambda_u(x) = \sum_i \lambda_{u,i} x^{i-1}$  (resp.,  $\rho_u(x) = \sum_i \rho_{u,i} x^{i-1}$ ),  $u \in \{y, z\}$ , where the nonnegative coefficients  $\lambda_{u,i}$  (resp.,  $\rho_{u,i}$ ) represent the fraction of edges emanating from a variable (resp., check) node of degree  $i$ . The code design rate is

$$R_u = 1 - \int_0^1 \rho_u(x) dx / \int_0^1 \lambda_u(x) dx.$$

### C. Decoding

Decoding proceeds according to the maximum *a posteriori* probability (MAP) rule at both receivers in order to minimize the probability of *coded bit* error. Let  $\mathbf{h}_{u,j}$  be the  $j$ th column of the parity-check matrix of the user- $u$  code

$$\mathbf{x} = \sqrt{\alpha P}(1 - 2\mathbf{c}_y) + \sqrt{(1-\alpha)P}(1 - 2\mathbf{c}_z)$$

be the transmitted signal (the superposition of the two codewords  $\mathbf{c}_y$  and  $\mathbf{c}_z$ ), and  $\mathbf{y}$  and  $\mathbf{z}$  be, respectively, the vector of the user- $Y$  and of the user- $Z$  channel outputs. The MAP estimate of the bit  $c_{y,i}$  at the user- $Y$  receiver is

$$\hat{c}_{y,i} = \arg \max_{b \in \{0, 1\}} \Pr[c_{y,i} = b | \mathbf{y}] \quad (7)$$

where  $\Pr[c_{y,i} = b | \mathbf{y}]$  is the conditional marginal of the joint probability

$$\begin{aligned} \Pr[\mathbf{c}_y, \mathbf{c}_z, \mathbf{y}] &= \sum_{\mathbf{c}_z, \mathbf{c}_y: \mathbf{c}_y, i = b} \prod_{u=y, z} \prod_{j=1}^{n-k_u} \chi_{\{\mathbf{c}_u \mathbf{h}_{u,j} = 0\}} \\ &\cdot \prod_{i=1}^n e^{-\frac{|y_i - A_i x_i|^2}{N_0}} \chi_{\{x_i = \sqrt{\alpha P}(1 - 2c_{y,i}) + \sqrt{(1-\alpha)P}(1 - 2c_{z,i})\}}. \end{aligned} \quad (8)$$

The decoding of the bit  $c_{z,i}$  at the user- $Z$  decoder is completely analogous and obtained by exchanging in (7) the subscripts “ $z$ ” for “ $y$ ” and the output pairs  $(z_i, B_i)$  for  $(y_i, A_i)$ . Fig. 3 shows the portion of the factor graph representing the joint probability in (7) relative to the  $i$ th pair of coded bits  $(c_{y,i}, c_{z,i})$ . The transmit symbol  $x_i$  (double circle) is related to the coded bit  $c_i$  (single circle) via the mapper (double square), which represents the codeword superposition. The coded bits are related to each other via the check nodes (single square) that represent the code parity-check equations. The symbol  $\mu_{u,i,j}$  (resp.,  $\xi_{u,i,j}$ ) indicates the log-likelihood ratio (LLR) messages *to* (resp., *from*) the  $i$ th variable node from (resp., to) the  $j$ th check node. The variable nodes are numbered from 1 to  $n$  while the check nodes from 0 to  $n-k$ , with the convention that 0 indicates the mapping node.

As in the single-user case, the MAP decoding rule is approximated by the *sum-product algorithm* [18] applied locally at each node of the graph in Fig. 3 and by iteratively exchanging messages, in the form of

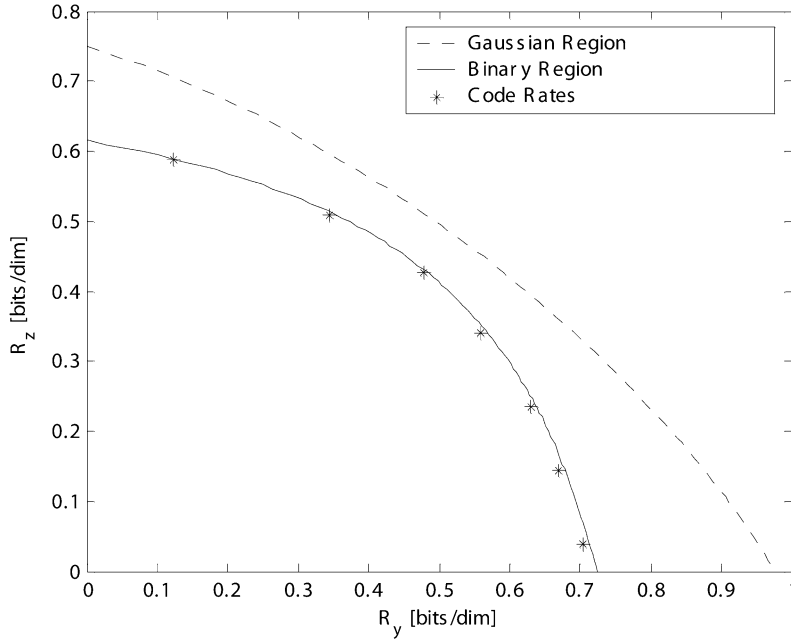


Fig. 1. Achievable regions and rates of the LDPC codes found for the unfaded BC with  $2|A|^2P/N_0 = 5.059$  dB and  $2|B|^2P/N_0 = 3.871$  dB.

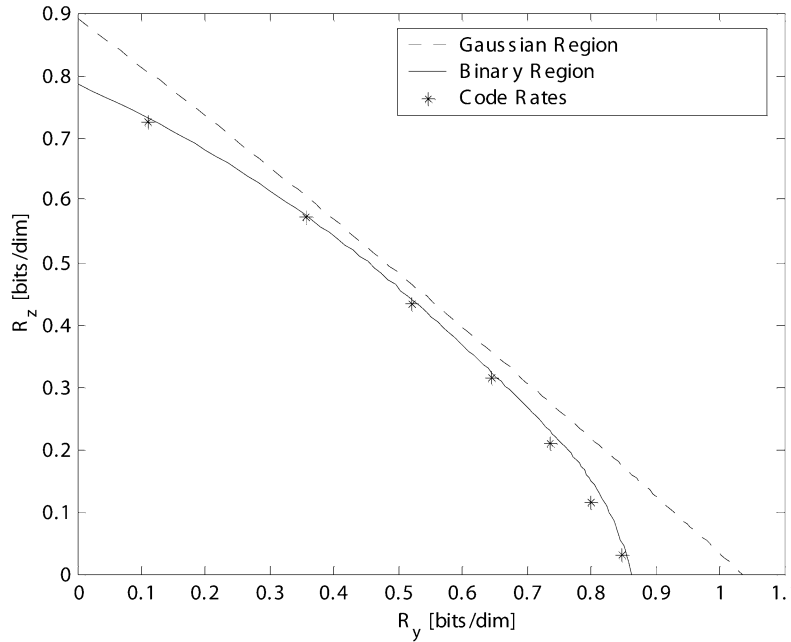


Fig. 2. Achievable regions and rates of the LDPC codes found for the Rayleigh fading BC with  $2E[|A|^2]P/N_0 = 3.098$  dB and  $2E[|B|^2]P/N_0 = 0.915$  dB.

LLRs, among the nodes. A possible schedule for the messages is as follows. At each iteration, messages are exchanged between variable nodes and check nodes on the subgraph of each user (on the left and on the right of the mapper node in Fig. 3) according to the standard message passing algorithm as described in [7]. However, before the next iteration on the user subgraphs begins, messages are exchanged through the mapper node. In particular, it can be shown that the LLR sent to the mapper is

$$\xi_{u,i,0} = \sum_{c>0} \mu_{u,i,c} \quad (9)$$

while the LLR sent by the mapper is

$$\mu_{u,i,0} = 2m_i\sqrt{\gamma_{u,i}} - 2\sqrt{\gamma_{y,i}\gamma_{z,i}}f(2m_i\sqrt{\gamma_{a,i}} + \xi_{a,i,0}, 2\sqrt{\gamma_{y,i}\gamma_{z,i}}) \quad (10)$$

where  $a \neq u \in \{y, z\}$ ,  $m_i = \text{Re}\{y_i/\sqrt{N_0/2}e^{-j\angle A_i}\}$  is the output of the user- $Y$  matched filter,  $\gamma_{u,i} = \alpha_u 2P|A_i|^2/N_0$  is the instantaneous received SNR of user- $u$  at the user- $Y$  receiver for  $\alpha_y = 1 - \alpha_z = \alpha \in [0, 1]$ , and where

$$f(x, t) \triangleq \frac{1}{t} \log \frac{\cosh((x+t)/2)}{\cosh((x-t)/2)}. \quad (11)$$

The algorithm terminates after  $\ell_{\max}$  iterations by outputting as bit estimate

$$\hat{c}_{u,i} = \chi \left\{ \mu_{u,i,0} + \sum_{j>0} \mu_{u,i,j} < 0 \right\}. \quad (12)$$

Notice that the first iteration on each user subgraph uses as “message from the channel” (10) computed for  $\xi_{a,i,0} = 0$ . Only when one of

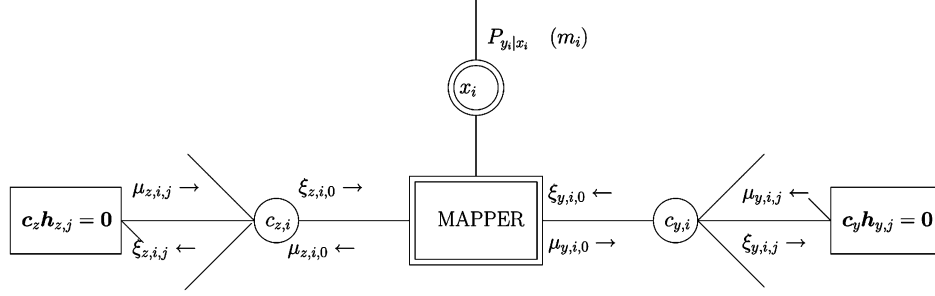


Fig. 3. Section of the factor graph referring to the  $i$ th pair of coded bits.

the users is allotted zero power the message in (10) reduces to a scaled version of the matched filter output  $2m_i\sqrt{\gamma_{u,i}}$ , as in the single-user case, and does not change with the iterations.

At the user- $Z$  decoder, the mapper node message is computed as in (10) but with  $(y_i, A_i)$  replaced by  $(z_i, B_i)$ .

#### D. The Mapper Node as an Interference Canceller

The flow of information through the mapper represented by (10) implies that a message referring to a particular user bit is influenced by the “reliability” of the other user bits. Because the bitwise MAP decoder in (7) is inherently a *single-user decoder*, the presence of the user- $Z$  codeword in the received signal is never beneficial. We therefore expect that the mapper node somehow performs the cancellation of the interference due to the other user codeword to enhance the reliability of the LLR messages.

The interpretation of the expression in (10) as soft-interference cancellation comes from the observation that the function in (11) is odd for any value of the parameter  $t$  and, for  $|x| \gg 1$ , it can be approximated as  $f(x, t) \approx \text{sign}(x)$ . Indeed,  $f(x, t)$  acts as a weighting function for the binary phase-shift keying (BPSK) symbol estimate “ $\text{sign}(x)$ ”: if  $|x| \ll 1$  then  $f(|x|, t) \approx 0$  since in this case, the estimate is unreliable; on the contrary, if  $|x| \gg 1$  then  $f(|x|, t) \approx 1$  since with high probability “ $\text{sign}(x)$ ” is the correct estimate.<sup>1</sup> Notice that “ $\text{sign}\{\xi_{z,i,0} + 2m_i\sqrt{\gamma_{z,i}}\}$ ” is the best hard estimate of the user- $Z$  transmitted symbol in a single-user perspective when the node is given the channel observation  $m_i$  and the sum of all the messages from the check nodes represented by  $\xi_{z,i,0}$  (recall the decision rule in (12).)

The mapper node viewed as an interference canceller explains why joint decoding of superimposed LDPC codes achieves “a general point in the two-user Gaussian MAC capacity without time sharing or rate splitting” [11]. In fact, with iterative decoding, the complexity of decoding a generic rate point of the dominant face is no more than the complexity of decoding any of the vertices, which can be achieved by subsequent single-user decoding and stripping. However, an optimal maximum-likelihood (ML) decoder performs one hard codeword cancellation per user while an iterative message-passing decoder performs ongoing soft bit cancellation. Although different from the theoretically optimal ML decoding with stripping, we shall next show that the iterative message-passing decoding achieves rate points extremely close to the achievable region of [5].

### III. PERFORMANCE ANALYSIS

The BER performance of the iterative message-passing decoding algorithm is exactly evaluated, in the limit for large block length  $n$ , by using the *density evolution* technique or can be visualized by using the

<sup>1</sup>The expression in (10), and its interpretation as soft bit interference canceller, generalizes to the  $K$ -user broadcast channel case, to the  $K$ -user multiple-access case, and to certain multilevel modulations such as  $M$ -PAM and square QAM.

*extrinsic information transfer (EXIT) chart* method. The former analytically tracks the evolution of the probability mass function of a randomly chosen message as the decoding progresses [7], [9], while the latter graphically tracks the evolution of a single parameter related to the density function [14].

Our goal is to find degree distributions  $(\lambda, \rho)$  which result in codes with vanishing BER as the block length and the number of iterations increase. We analyze the average performance of the LDPC  $(n, \lambda, \rho)$  ensemble for  $n \rightarrow \infty$  and we restrict attention to the cycle-free case as done in the single-user case [7]. In fact, the performance of each code in the ensemble converges to the average ensemble performance exponentially fast in the block length  $n$ , and each code is cycle free with probability  $(1 - O(1/n))$ . The proof of those facts follows the same steps, with some obvious modifications,<sup>2</sup> as their single-user counterparts.

#### A. The Stability Condition

As in [7], we shall assume that the graph representing the joint probability in (7) is cycle free and that  $\Phi_u^{(\ell-1)}$ , the density of the incoming message at a variable node from a check node at the  $(\ell-1)$ th iteration, conditioned on having transmitted the zero bit, is of the form

$$\Phi_u^{(\ell-1)} = (1 - \epsilon_u^{(\ell-1)}) \Delta_{+\infty}(x) + \epsilon_u^{(\ell-1)} \Delta_0(x) \quad (13)$$

where  $\Delta_a(x)$  indicates a mass point at  $x = a$  and where  $\epsilon_u^{(\ell-1)} \in [0, 1]$ . After a complete iteration, the density of the LLR message has evolved to

$$\Phi_u^{(\ell)} = \left[ (1 - \epsilon_u^{(\ell)}) \Delta_{+\infty}(x) + \epsilon_u^{(\ell)} \Delta_0(x) \right] \otimes Q_u(x) \quad (14)$$

where  $\otimes$  denotes the convolution and where

$$\epsilon_u^{(\ell)} = 1 - \rho_u \left( 1 - \lambda_u \left( \epsilon_a^{(\ell-1)} \right) \right) \quad (15)$$

$$Q_u(x) = \left( 1 - \epsilon_a^{(\ell-1)} \lambda_a \left( \epsilon_a^{(\ell-1)} \right) \right) Q_u^{(C)}(x) + \epsilon_a^{(\ell-1)} \lambda_a \left( \epsilon_a^{(\ell-1)} \right) Q_u^{(I)}(x), \quad u \neq a \quad (16)$$

i.e.,  $\epsilon_u^{(\ell)}$  in (15) is the probability that the LLR message at the  $\ell$ th iteration is zero,  $Q_u^{(C)}$  and  $Q_u^{(I)}$  are the densities of the message from the mapper when the reliability of the “interfering” user bit is, respectively, infinite and zero, conditioned on the user- $u$  bit being zero. The density in (16) depends on the fading and on the channel noise through matched filter output, i.e., through  $Q_u^{(C)}(x)$  and  $Q_u^{(I)}(x)$ . Moreover, in the evaluation of (14), only the user of interest is assumed to have sent the all-zero codeword while the other user is assumed to have transmitted a typical codeword composed with an equal number of zeros and ones, this fact is used in the evaluation of  $Q_u^{(I)}(x)$  ( $Q_u^{(C)}(x)$  is a Gaussian density as in the single-user case).

The iterative decoding process is said to converge if the bit-error probability vanishes for  $\ell^{(\max)} \rightarrow \infty$ . Since, by our convention, the channel seen by user- $Y$  is better than the channel seen by user- $Z$ , user- $Y$  can recover its message and the message intended for user- $Z$ .

<sup>2</sup>The proof of the cycle-free convergence for the entire graph hinges on seeing the two sets of variable nodes as coincident.

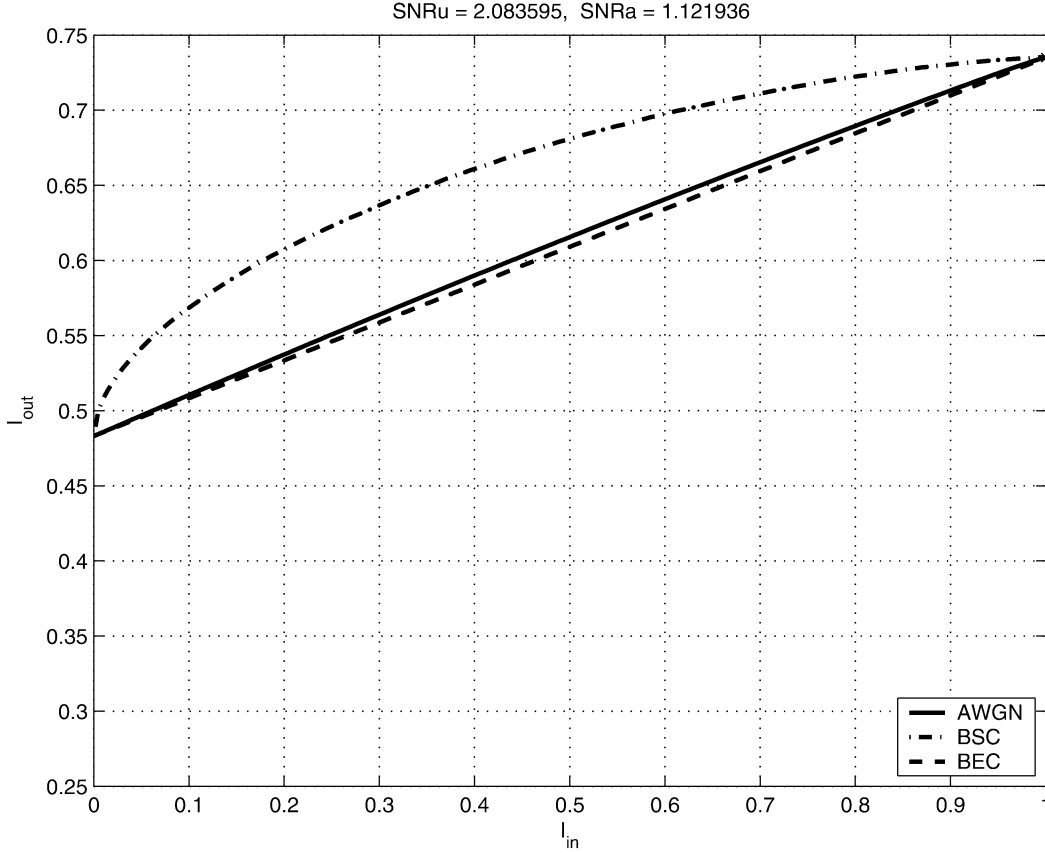


Fig. 4. Mapper transfer function from user- $Y$  to user- $Z$  for three different models of the extrinsic channel. User- $Y$  decoder for an unfaded BC with  $2|A|^2P/N_0 = 5.059$  dB and  $\alpha = 0.35$  resulting in  $I(X_y; Y) = 0.274$ ,  $I(X_y; Y|X_z) = 0.523$ ,  $I(X_z; Y) = 0.483$  and  $I(X_z; Y|X_y) = 0.735$ .

The stability condition is readily obtained by imposing that  $\epsilon_u^{(\ell-1)} \ll 1$  for both  $u = y$  and  $u = z$ . It then follows similarly to [9] that the probability of error decreases if

$$\frac{1}{\lambda'_u(0)\rho'_u(1)} > \int Q_u^{(C)}(t)e^{-t/2}dt = \mathbb{E}_A \left[ e^{-\frac{\gamma_u}{2}} \right] \quad (17)$$

where  $\gamma_u = 2|A|^2\alpha_u P/N_0$ . Hence, the stability condition at the decoder of the best user decouples into two independent “single-user” stability conditions, as for the MAC [11].

At the user- $Z$  receiver only the user- $Z$  codeword is reliably decoded. The stability condition, obtained by imposing  $\epsilon_z^{(\ell-1)} \ll 1$  and  $\epsilon_y^{(\ell-1)} \approx 1$  is

$$\begin{aligned} \frac{1}{\lambda'_z(0)\rho'_z(1)} &> \int Q_z^{(I)}(t)e^{-t/2}dt \\ &= \mathbb{E}_{N,B} \left[ e^{-\frac{\gamma_z}{2} - \frac{\gamma_y}{2}} \right. \\ &\quad \left. \cdot \sqrt{\frac{\cosh(2N\sqrt{\gamma_y}) + \cosh(2\sqrt{\gamma_y}\gamma_z)}{2}} \right] \quad (18) \end{aligned}$$

where (18) is the Bhattacharyya constant [9] of the channel  $f_{Z|s}(z) \sim s\sqrt{\gamma_z} + \sqrt{\gamma_y}X + \mathcal{N}_R(0, 1)$  for  $X \in \{\pm 1\}$  equally likely,  $N \sim \mathcal{N}_R(0, 1)$ , and  $\gamma_u = 2|B|^2\alpha_u P/N_0$ . We notice that (18) is well approximated in the high-SNR regime by the lower bound ( $\sqrt{\cosh(\sqrt{x}) + \alpha}$  is a convex-U function for  $\alpha \geq 1/2$ )

$$\mathbb{E}_B \left[ e^{-\frac{\gamma_z}{2} - \frac{\gamma_y}{2}} \sqrt{\frac{\cosh(2\sqrt{\gamma_y}) + \cosh(2\sqrt{\gamma_y}\gamma_z)}{2}} \right]$$

and by  $\mathbb{E}_B[e^{-\frac{1}{2} \frac{\gamma_z}{1+\gamma_y}}]$  in the low-SNR regime. It is worth noticing that the mean values in (17) and in (18) are computed with respect to two

different fading statistics as the channels seen by the two users are, in general, different.

### B. EXIT Chart Analysis

Following [12], we view the variable nodes as being repetition codes with respect to their edges, the check nodes as being single-parity check codes with respect to their edges, and the overall LDPC code as a concatenation of those codes. The performance of such a concatenated scheme can be analyzed using the EXIT chart method.

Let  $G_\lambda(x, y)$  be the polynomial

$$G_\lambda(x, y) \triangleq \sum_i \lambda_i J((i-1)J^{-1}(x) + J^{-1}(y)) \quad (19)$$

defined for  $(x, y) \in [0, 1] \times [0, 1]$  and for  $J(x)$  in (6). For  $u \in \{y, z\}$ , let  $I_{m,u}$ ,  $I_{v,u}$ , and  $I_{c,u}$  denote the mutual information between bit  $X_u$  of user- $u$  and, respectively, the message from the mapper to a variable node, the message from a variable node to a check node, and the message from a check node to a variable node. By using the “Gaussian approximation” for incoming messages [12], and the “duality property” [15], the different mutual informations relate to each other as

$$I_{v,u} = G_{\lambda_u}(I_{c,u}, I_{m,u}) \quad (20)$$

$$I_{c,u} = 1 - G_{\rho_u}(1 - I_{v,u}, 0). \quad (21)$$

In a single-user setting,  $I_{m,u}$  equals the mutual information between a coded bit and the corresponding channel output, that is,  $I_{m,u} = I(X; Y)$ . In this case, subject to the approximations inherent in EXIT chart methods, reliable decoding is possible if

$$1 - G_{\rho_u}(1 - G_{\lambda_u}(x, I_{m,u}), 0) > x \quad (22)$$

for all  $x \in [0, 1)$ . In a multiuser setting,  $I_{m,u}$  depends on the channel output and on the reliability of the other user’s bits. We shall therefore extend the idea of (22) to track the evolution of the mutual information

TABLE I  
DEGREE DISTRIBUTION PAIRS FOR THE USER-Z CODE FOR AN UNFADED CHANNEL WITH  $2|B|^2P/N_0 = 3.871$  dB  
TOGETHER WITH THE ASSOCIATED DESIGN RATES AND RECEIVE SNR IN DECIBELS

$\alpha$	0.05	0.20	0.35	0.50	0.65	0.80	0.95
$\lambda_2$	0.03323	0.08516	0.13259	0.18100	0.23913	0.31907	0.48415
$\lambda_3$	0.39055	0.34820	0.32749	0.30972	0.29443	0.27252	0.21485
$\lambda_6$							0.07009
$\lambda_7$						0.01974	0.11266
$\lambda_8$					0.08601	0.20539	
$\lambda_9$				0.19343	0.15901		
$\lambda_{10}$	0.00047	0.13366	0.26180	0.06225			
$\lambda_{11}$	0.05477	0.07619	0.00377				
$\lambda_{12}$	0.22054	0.05732					
$\lambda_{49}$	0.00235	0.00120	0.00038	0.00040	0.00017	0.00028	
$\lambda_{50}$	0.29809	0.29827	0.27397	0.25320	0.22125	0.18300	0.11825
$\rho_3$						0.00004	1.00000
$\rho_4$						0.99996	
$\rho_5$					0.95237		
$\rho_6$				0.53070	0.04763		
$\rho_7$				0.46922			
$\rho_8$			0.45642				
$\rho_9$			0.54356				
$\rho_{12}$		0.69672		0.00002			
$\rho_{13}$		0.29874	0.00002	0.00006			
$\rho_{15}$		0.00196					
$\rho_{16}$		0.00248					
$\rho_{20}$	0.47834	0.00010					
$\rho_{21}$	0.50459						
$\rho_{25}$	0.00394						
$\rho_{26}$	0.01313						
R	0.7242	0.5712	0.4338	0.3136	0.2081	0.1151	0.0305
$\gamma_z$ dB	3.6482	2.9019	2.0001	0.8607	-0.6883	-3.1187	-9.1393

relative to the bits of *both* users by finding an appropriate expression for  $I_{m,u}$ .

The mutual information between a bit  $X_z$  and the message  $M$  from a user- $Z$  variable node to the mapper, derived similarly to (20), is

$$I_{z \rightarrow m} = G_{\lambda_z}(I_{c,z}, I_{c,z}). \quad (23)$$

The mutual information between a bit  $X_y$  and a message from the mapper, a function of the channel output  $Y$ , and the message  $M$  from the other user, can be evaluated as

$$I_{m,y} = I(X_y; Y|M) = 1 - \mathbb{E}[\log_2(1 + e^{-T})] \quad (24)$$

where  $T$  is a random variable distributed as the message from the mapper in (10), for  $\xi = M$ , given that  $X_y = 1$  and that  $M$  is the bit  $X_z$  observed through a Gaussian channel with SNR  $J^{-1}(I_{z \rightarrow m})$  for  $I_{z \rightarrow m}$  as in (23). Fig. 4 shows the mapper node transfer function  $I_{m,z}$  versus  $I_{c,y}$  for the codes in Tables I and II with  $\alpha = 0.35$  (we plot  $I_{m,z}$  versus  $I_{c,y}$ , instead of  $I_{m,y}$  versus  $I_{c,z}$ , to highlight cases where the BEC and the additive white Gaussian noise modeled extrinsic channel give notably different results.) From Fig. 4 we notice that  $I_{m,z}$  is almost a linear function, i.e.,  $I_{m,z} \approx \theta_{z,Y}(I_{c,y})$  for  $\theta_{u,Y}(I_{c,a})$  (the first subscript indicates the user and the second the channel)

$$\theta_{u,Y}(I_{c,a}) = I_{a \rightarrow m} I(X_u; Y|X_a) + (1 - I_{a \rightarrow m}) I(X_u; Y) \quad (25)$$

as if  $M$  was the output of a BEC with erasure probability  $1 - I_{y \rightarrow m}$ .<sup>3</sup> However, the expression in (25) does not seem to be in general a firm bound, in the sense of the BEC being the “least informative channel” [19], [20] for the mapper node. From numerical evaluations it turns out that (25) is a very good approximation of (24) for a wide range

<sup>3</sup>Since  $M$  is a noisy observation of  $X_z$  only, we have

$$I(X_y; Y|M) \in [I(X_y; Y), I(X_y; Y|X_z)].$$

of SNRs, i.e., failing only when the two SNRs are significantly different. Hence, in our EXIT chart analysis, we shall use (25) as the mapper node transfer function. Notice that (25) depends on the physical channel (fading) only through  $I(X_u; Y|X_a)$  and  $I(X_u; Y)$ .

By putting together (20), (21), and (25), we conclude that the multiuser equivalent of (22) for joint decoding at the user- $Y$  receiver is that  $x_y^{(\ell+1)} \rightarrow 1$  as  $\ell \rightarrow \infty$  where

$$x_y^{(\ell+1)} = 1 - G_{\rho_y} \left( 1 - G_{\lambda_y} \left( x_y^\ell, \theta_{y,Y}(x_z^\ell) \right), 0 \right) \quad (26a)$$

$$x_z^{(\ell+1)} = 1 - G_{\rho_z} \left( 1 - G_{\lambda_z} \left( x_z^\ell, \theta_{z,Y}(x_y^\ell) \right), 0 \right) \quad (26b)$$

while the condition for single-user decoding at the user- $Z$  receiver is (22) for  $u = z$  and  $I_{m,u} = \theta_{z,Z}(0) = I(X_z; Z)$ . Figs. 5 and 6 show (26a) and (26b) versus  $(x_y^\ell, x_z^\ell)$ . It is interesting to notice that  $x_y^{(\ell+1)}$  need not be always above  $x_y^{(\ell)}$  to assure convergence. In a way, at the beginning of the decoding process at the user- $Y$  receiver, the user- $Y$  code operates at an SNR below its threshold. Only when part of the interference from the user- $Z$  code has been removed the user- $Y$  code operates at an SNR which allows the decoding process to progress and eventually successfully converge.

### C. Code Optimization

We simplify the code search by first finding a “good” user- $Z$  code and then optimizing the user- $Y$  code, given the found user- $Z$  code. Our optimization algorithm is as follows. We enforce our candidate codes to fulfill the conditions in (17) and (18). For a fixed degree distribution, we use the EXIT chart method to determine the (approximate) threshold of the corresponding LDPC ensembles by verifying conditions (26) and (22) for a fixed channel. Then, by using the differential evolution algorithm [9], [10], we modify the found degree distributions and we check whether the new ones have a higher rate while ensuring that (26) and (22) are still satisfied. We then iteratively repeat this process.

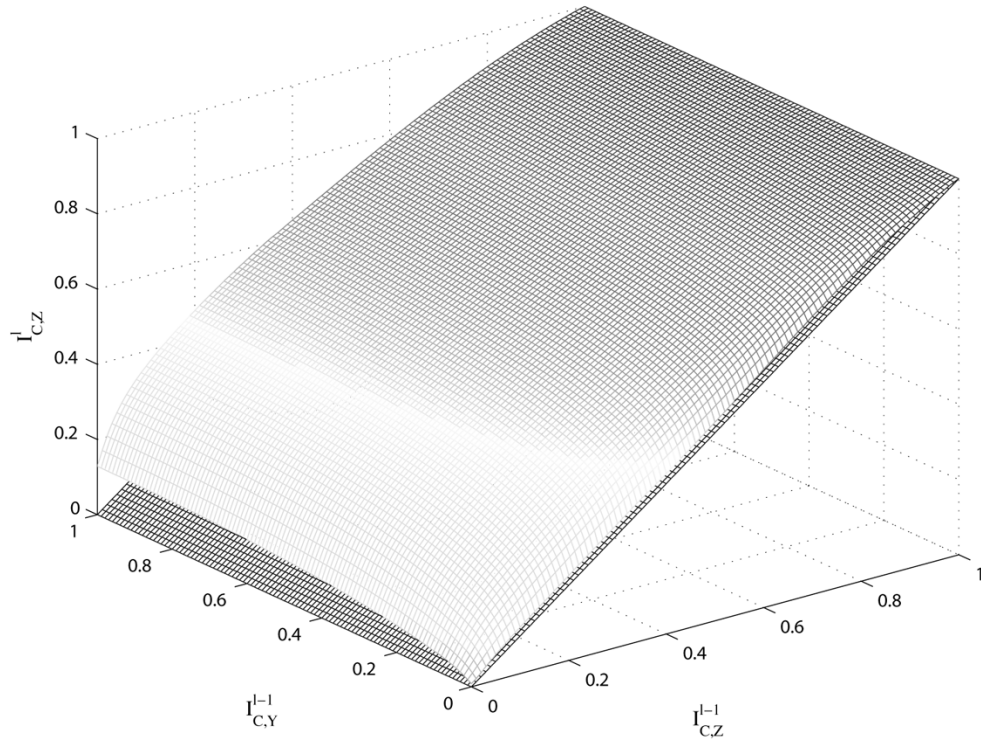


Fig. 5. Evolution of the user-Z mutual information  $I_{z,c}^{(\ell)}$  as function of  $I_{z,c}^{(\ell-1)}$  and  $I_{y,c}^{(\ell-1)}$  for the codes in Tables I and II for  $\alpha = 0.35$ . Also represented for comparison the plane  $I_{z,c}^{(\ell)} = I_{z,c}^{(\ell-1)}$ .

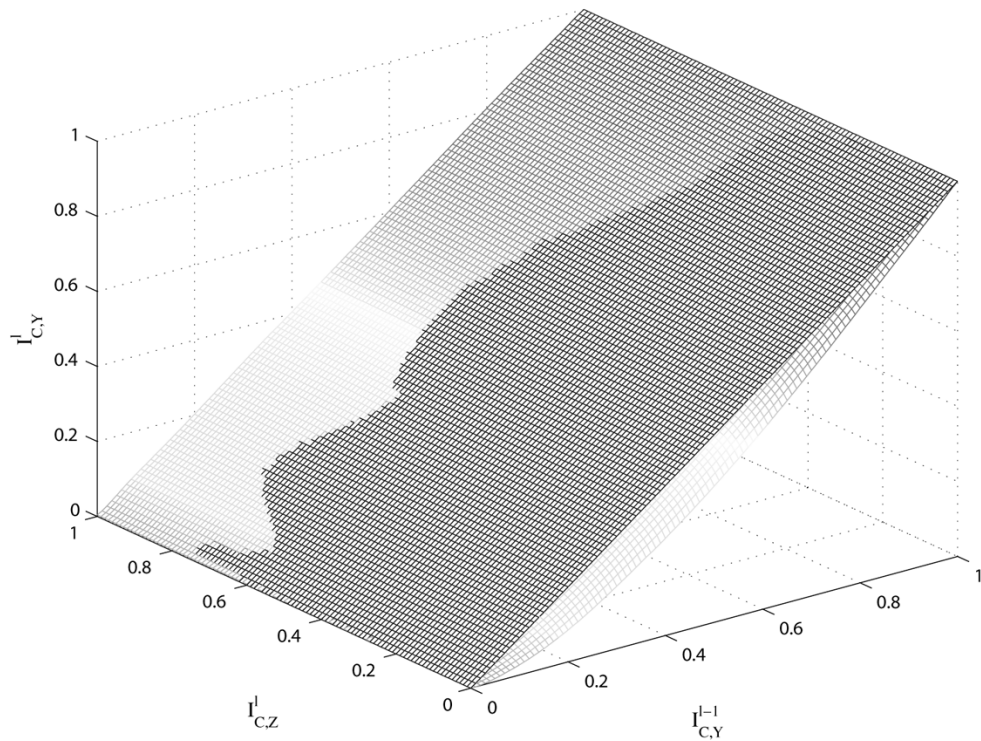


Fig. 6. Evolution of the user-Y mutual information  $I_{y,c}^{(\ell)}$  as function of  $I_{z,c}^{(\ell-1)}$  and  $I_{y,c}^{(\ell-1)}$  for the codes in Tables I and II for  $\alpha = 0.35$ . Also represented for comparison the plane  $I_{y,c}^{(\ell)} = I_{y,c}^{(\ell-1)}$ .

*D. Numerical Results*

Using the above mentioned code search procedure, we found LDPC codes with (approximate) SNR thresholds close to their Shannon limit for both unfaded and Rayleigh-fading channels. For each channel, we

considered several values of  $\alpha \in [0, 1]$  each corresponding to a different power share and hence resulting in a different rate point. Tables I and II show, respectively, the degree distributions for the user-Z codes and the user-Y codes for an unfaded channel with  $|B|^2 P/N_0 = 3.871$  dB and  $|A|^2 P/N_0 = 5.059$  dB. Tables III and IV show the de-

TABLE II  
DEGREE DISTRIBUTIONS PAIRS FOR THE USER- $Y$  CODE FOR AN UNFADED CHANNEL WITH  $2|A|^2P/N_0 = 5.059$  dB  
AND THE CORRESPONDING DESIGN RATES AND RECEIVE SNR WHEN PAIRED WITH THE  
CODES IN TABLE I

$\alpha$	0.05	0.20	0.35	0.50	0.65	0.80	0.95
$\lambda_2$	0.34249	0.20810	0.16775	0.14690	0.13612	0.12454	0.11620
$\lambda_3$	0.22816	0.21403	0.19545	0.18959	0.17964	0.18387	0.18737
$\lambda_7$	0.15017				0.03831		
$\lambda_8$	0.09710	0.20353	0.22167	0.15951	0.21937	0.18481	0.03361
$\lambda_9$		0.09300	0.08149	0.15282		0.08404	0.28038
$\lambda_{12}$						0.03366	
$\lambda_{13}$					0.06743	0.01960	
$\lambda_{14}$					0.00393		
$\lambda_{49}$				0.00013	0.00013	0.00019	0.00014
$\lambda_{50}$	0.18217	0.28134	0.33366	0.35105	0.35507	0.36938	0.38230
$\rho_3$	0.04844						
$\rho_4$	0.93647						
$\rho_5$	0.01509						
$\rho_7$		0.83234					
$\rho_8$		0.16766					
$\rho_{10}$			0.12033				
$\rho_{11}$			0.87967				
$\rho_{15}$				0.34069			
$\rho_{16}$				0.65931	0.17856		
$\rho_{21}$					0.82144		
$\rho_{29}$						0.05470	
$\rho_{30}$						0.94530	
$\rho_{40}$							0.55678
$\rho_{41}$							0.43172
$\rho_{42}$							0.01148
R	0.1098	0.3548	0.5219	0.6461	0.7356	0.8008	0.8488
$\gamma_y$ dB	-7.9510	-1.9304	0.5000	2.0490	3.1885	4.0902	4.8366

TABLE III  
DEGREE DISTRIBUTION PAIRS FOR THE USER- $Z$  CODE FOR A RAYLEIGH FADING CHANNEL WITH  $2E[|B|^2]P/N_0 = 0.915$  dB  
TOGETHER WITH THE ASSOCIATED DESIGN RATES AND RECEIVE SNR IN DECIBELS

$\alpha$	0.05	0.20	0.35	0.50	0.65	0.80	0.95
$\lambda_2$	0.10848	0.13262	0.15836	0.18945	0.23855	0.29875	0.47105
$\lambda_3$	0.29099	0.28618	0.27978	0.27354	0.26381	0.25018	0.22087
$\lambda_6$							0.02513
$\lambda_7$						0.12075	0.16201
$\lambda_8$				0.04376	0.21037	0.11344	
$\lambda_9$	0.12258	0.12749	0.21662	0.22855	0.04610		
$\lambda_{10}$	0.14729	0.15215	0.06069	0.00017			
$\lambda_{31}$					0.00002		
$\lambda_{49}$	0.00016	0.00025	0.00025	0.00002	0.00002	0.00004	0.00004
$\lambda_{50}$	0.33050	0.30131	0.28450	0.26451	0.24113	0.21684	0.12090
$\rho_3$							0.90982
$\rho_4$						0.59843	0.09018
$\rho_5$					0.58790	0.40156	
$\rho_6$				0.14880	0.41207		
$\rho_7$				0.85117		0.00001	
$\rho_8$			0.597005		0.00001		
$\rho_9$			0.402207		0.00002		
$\rho_{10}$		0.65254					
$\rho_{11}$		0.34728	0.000663				
$\rho_{12}$			0.000125				
$\rho_{13}$	0.98284						
$\rho_{14}$	0.01716	0.00003					
$\rho_{15}$		0.00009					
$\rho_{16}$		0.00004		0.00001			
$\rho_{17}$				0.00002			
R	0.58738	0.50872	0.42677	0.34079	0.23491	0.14380	0.038597
$\gamma_z$ dB	0.6922	-0.0541	-0.9559	-2.0953	-3.64432	-6.07470	-12.09530

gree distributions for a Rayleigh-fading channel with  $E[|B|^2]P/N_0 = 0.915$  dB and  $E[|A|^2]P/N_0 = 3.098$  dB. Figs. 2 and 3 show the achievable rate regions for binary input and the optimized code rate pairs. The code rate pairs are very close to the boundary of the achievable region for both channel models.

We notice that codes with higher maximum variable node degree have lower SNR thresholds, as remarked in [9]. Intuition would indeed agree that codes whose bits are involved in more parity-check equations offer greater reliability. Our code search shows that, similarly to what [21], has been observed for erasure channels Gaussian channels [9],



TABLE IV  
DEGREE DISTRIBUTIONS PAIRS FOR THE USER- $Y$  CODE FOR THE RAYLEIGH FADING CHANNEL WITH  $2E[|A|^2]P/N_0 = 3.098$  dB AND THE CORRESPONDING DESIGN RATES AND RECEIVE SNR WHEN PAIRED WITH THE CODES IN TABLE III

$\alpha$	0.05	0.20	0.35	0.50	0.65	0.80	0.95
$\lambda_2$	0.27889	0.20954	0.16947	0.12516	0.14584	0.14028	0.13430
$\lambda_3$	0.23153	0.21972	0.23080	0.17892	0.19828	0.19498	0.19517
$\lambda_8$	0.27307	0.19718	0.03293	0.12806	0.12864	0.11963	0.08830
$\lambda_9$	0.00388	0.09472	0.27853	0.15040	0.18192	0.19204	0.22545
$\lambda_{36}$			0.00004				
$\lambda_{49}$	0.00030	0.00012	0.00087	0.00017	0.00036	0.00021	0.00220
$\lambda_{50}$	0.21233	0.27872	0.28736	0.41729	0.34496	0.35286	0.35458
$\rho_3$	0.13124			0.01637			
$\rho_4$	0.13209			0.00240			
$\rho_5$	0.73304						
$\rho_6$	0.00363	0.01718					
$\rho_7$		0.98282					
$\rho_8$			0.04171				
$\rho_9$			0.42127				
$\rho_{10}$			0.53702				
$\rho_{14}$				0.15606	0.12771		
$\rho_{15}$				0.82517	0.87229		
$\rho_{16}$						0.07055	
$\rho_{17}$						0.92945	
$\rho_{19}$							0.66295
$\rho_{20}$							0.33705
R	0.12315	0.34510	0.47790	0.55774	0.63079	0.66898	0.70504
$\gamma_y$ dB	-9.91226	-3.89166	-1.46128	0.08774	1.22717	2.12894	2.87528

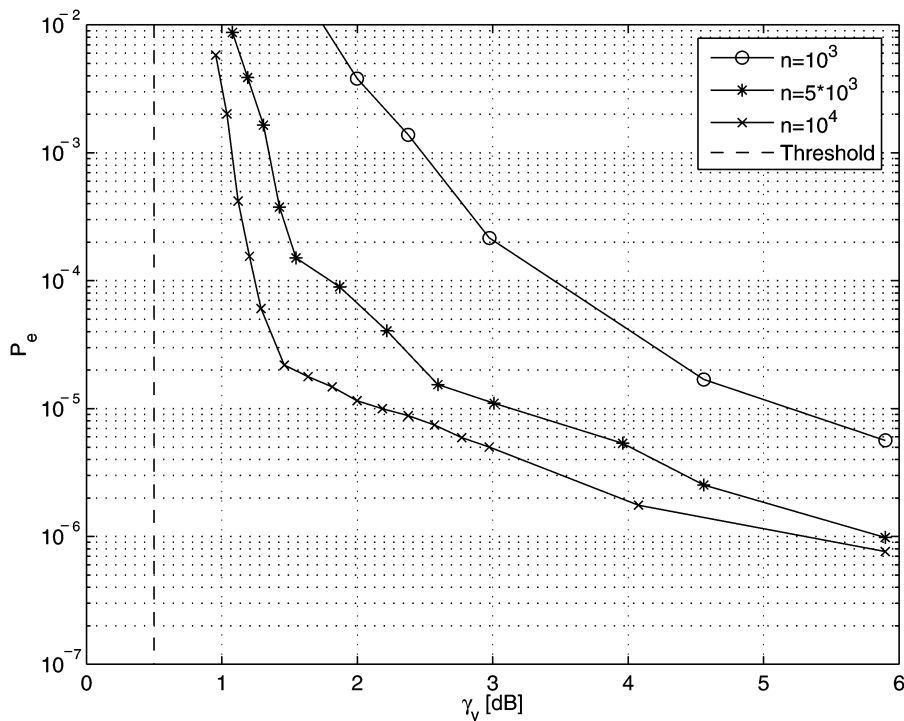


Fig. 7. User- $Y$  BER (over systematic bits only) for joint decoding of the codes in Tables I and II for  $\alpha = 0.35$  and finite block length.

and uncorrelated Rayleigh-fading Gaussian channels [10], the optimized degree distributions have only a few nonzero terms. The variable node degrees tend to be concentrated around the maximum allowable degree, the degree two, and a few other degrees in between. The check node degrees are concentrated around a single degree whose value depends on the average receive SNR. Also, the overall form of the degree distributions are similar for the unfaded and the fading case.

The concentration theorem [7] ensures that for sufficiently large block length almost every code in the ensemble will have vanishing probability of error, if the receive SNR is above the ensemble threshold.

This condition was enforced in our code search. However, we are also interested in the code performance for finite block lengths. Fig. 7 shows the BER performance of the codes in Table I and in Table II with block length  $n = 10^3$ ,  $5 \cdot 10^3$  and  $n = 10^4$ . The degree distributions were optimized for an unfaded channel with  $2|B|^2P/N_0 = 3.871$  dB,  $2|A|^2P/N_0 = 5.059$  dB, and  $\alpha = 0.35$ . We notice that the threshold effect is already quite pronounced at a block length of  $n = 10^4$ .

One of the anonymous reviewers pointed out that the poor performance of the  $n = 10^3$  ensemble is likely due to unavoidable length-4 cycles. Here our goal is to show the effectiveness of LDPC codes on

general fading BCs and not to design optimized finite-length codes, for which criteria other than the asymptotic performance must be considered.

#### IV. CONCLUSION

In this work we studied the performance of LDPC codes on two-user Gaussian BCs with fading.

In applying the sum-product update rule to deriving the joint message-passing decoding algorithm, we found that the message update rule at the mapping node linking the users' codes is equivalent to soft interference cancellation. Interestingly, a low-complexity implementation of the optimal update rule at the mapper is equivalent to hard interference cancellation.

We showed that good degree distribution pairs can be found to approach the Shannon limit for binary constrained input BCs. We computed the stability condition that the pair of codes must satisfy in order to ensure vanishing probability of error for large block length and infinite iterations by using the expression based on the Bhattacharyya distance between the two channel transition probabilities. We show that the overall stability condition is actually composed of *three* conditions: two for reliable joint decoding at the best receiver and one for reliable single-user decoding at the worst receiver. We enforced these conditions when optimizing the degree distributions by using a combination of the EXIT chart method and the differential evolution algorithm.

We also extended the EXIT chart method to account for the information coming from the other user's code. We propose an approximation of the mapper node transfer function based on the assumption of the extrinsic channel being a BEC. By simulation, we verified that this approximation is very tight for a wide range of SNRs in the Gaussian channel case.

We finally showed by simulations that the optimized codes can operate at about 1 dB from their threshold for finite block length.

#### ACKNOWLEDGMENT

The authors would like to thank Abdelaziz Amraoui for insightful discussions and the anonymous reviewers for their helpful comments and suggestions.

#### REFERENCES

- [1] T. M. Cover, "Broadcast channels," *IEEE Trans. Inf. Theory*, vol. IT-18, no. 1, pp. 2–14, Jan. 1972.
- [2] —, "Comments on broadcast channels," *IEEE Trans. Inf. Theory*, vol. 44, no. 6, pp. 2524–2530, Oct. 1998.
- [3] T. M. Cover and J. Thomas, *Elements of Information Theory*. New York: Wiley, 1991.
- [4] A. A. El Gamal, "The capacity of a class of broadcast channels," *IEEE Trans. Inf. Theory*, vol. IT-25, no. 2, pp. 166–169, Mar. 1979.
- [5] D. Tuninetti and S. Shamai (Shitz), "Gaussian broadcast channels with state information at the receivers," in *Proc. DIMACS Workshop on Network Information Theory*, Piscataway, NJ, Mar. 2003.
- [6] R. G. Gallager, *Low-Density Parity-Check Codes*. Cambridge, MA: MIT Press, 1963.
- [7] T. J. Richardson and R. L. Urbanke, "The capacity of low-density parity-check codes under message-passing decoding," *IEEE Trans. Inf. Theory*, vol. 47, no. 2, pp. 599–618, Feb. 2001.
- [8] R. McEliece, "The effectiveness of turbo-like codes on nonstandard channel models," presented at the IEEE International Symposium on Information Theory (ISIT 2001); Planary Talk, Washington, DC, Jun. 2001.
- [9] T. J. Richardson, M. A. Shokrollahi, and R. L. Urbanke, "Design of capacity-approaching irregular low-density parity-check codes," *IEEE Trans. Inf. Theory*, vol. 47, no. 2, pp. 619–637, Feb. 2001.
- [10] J. Hou, P. H. Siegel, and L. B. Milstein, "Performance analysis and code optimization of low density parity-check codes on Rayleigh fading channels," *IEEE J. Sel. Areas Commun.*, vol. 19, no. 5, pp. 924–934, May 2001.
- [11] A. Amraoui, S. Dusad, and R. Urbanke, "Achieving general points in the 2-user Gaussian MAC without time-sharing or rate-splitting by means of iterative coding," in *Proc. IEEE Int. Symp. Information Theory (ISIT 2002)*, Lausanne, Switzerland, Jun./Jul. 2002, p. 334.
- [12] S. ten Brink, G. Kramer, and A. Ashikhmin, "Design of low-density parity-check codes for modulation and detection," *IEEE Trans. Commun.*, vol. 52, no. 4, pp. 670–678, Apr. 2004.
- [13] A. Amraoui, G. Kramer, and S. Shamai (Shitz), "Coding for the MIMO broadcast channel," in *Proc. IEEE Int. Symp. Information Theory (ISIT 2003)*, Yokohama, Japan, Jun./Jul. 2003, p. 296.
- [14] S. ten Brink, "Convergence of iterative decoding," *Electron. Lett.*, vol. 35, pp. 806–808, May 1999.
- [15] A. Ashikhmin, G. Kramer, and S. ten Brink, "Extrinsic information transfer functions: Model and erasure properties," *IEEE Trans. Inf. Theory*, vol. 50, no. 11, pp. 2657–2673, Nov. 2004.
- [16] T. J. Richardson and R. L. Urbanke. (2005) Modern Coding Theory. [Online]. Available: <http://lthcwww.epfl.ch/mct/>
- [17] S. Verdú, G. Caire, and D. Tuninetti, "Is TDMA optimal in the low power regime?," in *Proc. IEEE Int. Symp. Information Theory (ISIT 2002)*, Lausanne, Switzerland, Jun./Jul. 2002, p. 193.
- [18] F. R. Kschischang, B. J. Frey, and H.-A. Loeliger, "Factor graphs and the sum-product algorithm," *IEEE Trans. Inf. Theory*, vol. 47, no. 2, pp. 498–519, Feb. 2001.
- [19] I. Sutskever, S. Shamai (Shitz), and J. Ziv, "Extremes in information combining," in *Proc. 4th ETH—Technion Information Theory Workshop*, Zurich, Switzerland, Feb. 2004.
- [20] I. Land, S. Huettinger, P. A. Hoeher, and J. B. Huber, "Bounds on information combining," *IEEE Trans. Inf. Theory*, vol. 51, no. 2, pp. 612–619, Feb. 2005.
- [21] A. Shokrollahi and R. Storn, "Design of efficient erasure codes with differential evolution," in *Proc. IEEE Int. Symp. Information Theory*, Sorrento, Italy, Jun./Jul. 2000, p. 5.